Title

Direct-Write, Self-Aligned Electrospinning on Paper for Controllable Fabrication of Three-Dimensional Structures.

Journal

ACS applied materials & interfaces, 7(50)

ISSN

1944-8244

Authors

Luo, Guoxi
Teh, Kwok Siong
Liu, Yumeng
et al.

Publication Date

2015-12-01

DOI

10.1021/acsami.5b08909

Peer reviewed

ACS APPLIED MATERIALS & INTERFACES

Research Article

www.acsami.org

Direct-Write, Self-Aligned Electrospinning on Paper for Controllable Fabrication of Three-Dimensional Structures

Guoxi Luo,[†,‡] Kwok Siong Teh,[*,‡,§] Yumeng Liu,[‡] Xining Zang,[‡] Zhiyu Wen,[†] and Liwei Lin[*,‡]

[†]College of Optoelectronic Engineering, Chongqing University, Chongqing 400044, China

[‡]Department of Mechanical Engineering, University of California, Berkeley, California 94720, United States

[§]School of Engineering, San Francisco State University, San Francisco, California 94132, United States

ABSTRACT: Electrospinning, a process that converts a solution or melt droplet into an ejected jet under a high electric field, is a well-established technique to produce one-dimensional (1D) fibers or two-dimensional (2D) randomly arranged fibrous meshes. Nevertheless, the direct electrospinning of fibers into controllable three-dimensional (3D) architectures is still a nascent technology. Here, we apply near-field electrospinning (NFES) to directly write arbitrarily shaped 3D structures through consistent and spatially controlled fiber-by-fiber stacking of polyvinylidene fluoride (PVDF) fibers. An element central to the success of this 3D electrospinning is the use of a printing paper placed on the grounded conductive plate and acting as a fiber collector. Once deposited on the paper, residual solvents from near-field electrospun fibers can infiltrate the paper substrate, enhancing the charge transfer between the deposited fibers and the ground plate via the fibrous network within the paper. Such charge transfer grounds the deposited fibers and turns them into locally fabricated electrical poles, which attract subsequent in-flight fibers to deposit in a self-aligned manner on top of each other. This process enables the design and controlled fabrication of electrospun 3D structures such as grids, walls, hollow cylinders, and other 3D logos. As such, this technique has the potential to advance the existing electrospinning technologies in constructing 3D structures for biomedical, microelectronics, and MEMS/NMES applications.

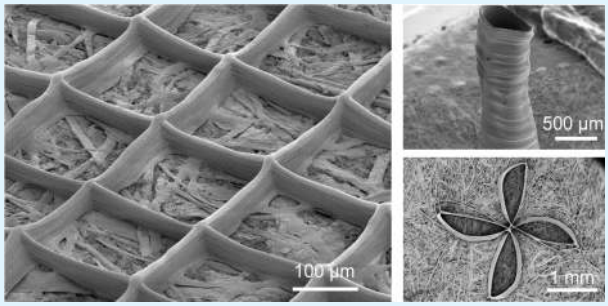

KEYWORDS: *3D electrospinning, 3D micro-/nanofabrications, direct-write, self-alignment, near-field electrospinning*

1. INTRODUCTION

Electrospinning, a technique that enables the production of continuous micro-/nanoscale fibers from solutions or melts under a high electric field, has come a long way since its invention in 1934.[1] In recent decades, the electrospinning process has attracted growing interest, triggered by the myriad potential applications of nanofibers in nanotechnology.[2,3] Electrospinning makes possible the construction of long and continuous polymeric,[4,5] ceramic,[6,7] and composite[8−10] fibers, thereby enabling their broad applications in tissue engineering,[11] medicine,[12] filtrations,[13] sensing,[14] field effect transistors,[15,16] transparent electrodes,[17] lithium-ion batteries,[18] supercapacitors,[19] and nanogenerators,[20] to name a few. In the biological field, for instance, electrospun fibers can be used to construct tissue engineering scaffolds, given their fibrous and porous structures, which closely mimic the morphological properties of the native extracellular matrix.[11] That being said, a desirable tissue scaffold is required to be a 3D mesoporous structure to sustain, guide, and facilitate the growth of desired functional tissues.[21,22] However, due to the bending instabilities[23] that are inherent to the electrospinning process, the final forms of electrospun fibers are generally collected as 2D randomly arranged meshes,[24,25] which inevitably restricts existing applications of electrospun fibers and the development of new applications.

Several methods for out-of-plane deposition of electrospun structures have been demonstrated in recent years. Among these methods, the technique of melt electrospinning can reduce the influence of bending instability, with improved control over fibers deposition, making it possible to deposit fibers in a layer-by-layer manner for producing 3D fibrous scaffolds.[21,26−30] Nevertheless, since melt electrospinning is based solely on simple repetitive stacking of fibers, the consistent fiber-by-fiber stacking for precise 3D construction is still difficult due to the lack of a precise spatial control mechanism over the alignment and stacking of electrospun fibers.[31,32] Furthermore, due to the higher viscosity and lower conductivity, melt-electrospun fibers generally tend to have much larger diameter than solution-electrospun fibers, limiting the further improvement of this technique in terms of resolution. Another methodology utilizes the technique of prefabricated ground collector to produce 3D electrospun architectures, such as tube-shaped structures through coiling fibers on top of a sharp conductive tip[33] and free-standing walls deposited on a prepatterned ground electrode.[34] Through manipulating electric field and electric forces with modification

Received: September 21, 2015
Accepted: November 23, 2015
Published: November 23, 2015

DOI: 10.1021/acsami.5b08909
ACS Appl. Mater. Interfaces 2015, 7, 27765−27770

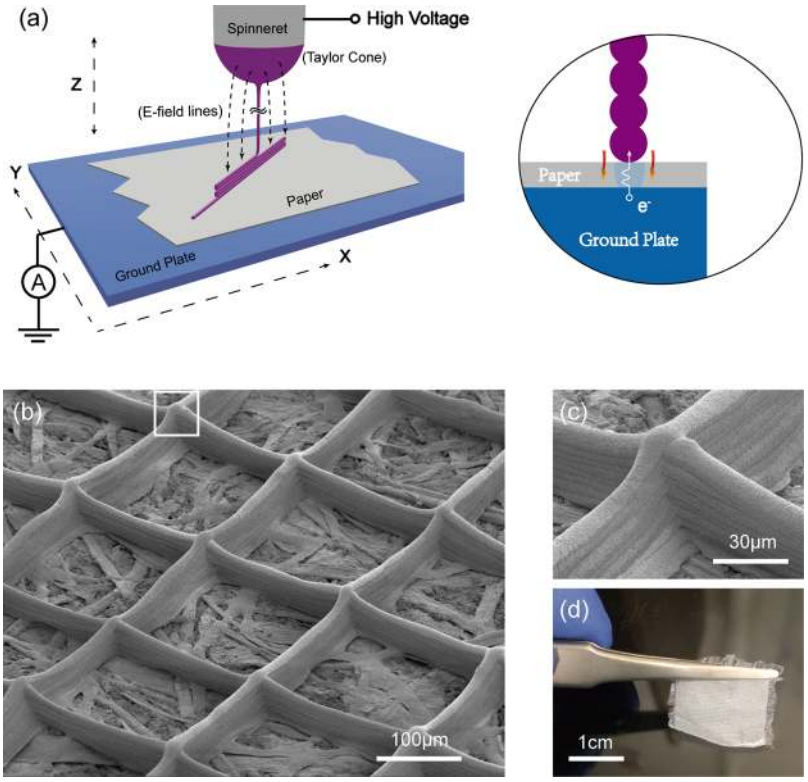

Figure 1. (a) Schematic setup of the 3D electrospinning process and a close-up schematic of stacked fibers. (b) SEM image of a 10-layer, 3D grid structure constructed on a paper substrate, with the following electrospinning parameters: spinneret size of 30 G, applied voltage at 1.5 kV, motion speed of 25 mm/s, and initial spinneret-to-collector distance of 1 mm. (c) SEM image showing the crossover area of the grid. (d) An optical photo showing a whole grid structure held by a tweezer after being physically detached from the paper substrate.

and prepatterning of the grounded collectors, these methods are capable of guiding the accurate deposition of electrospun fibers to produce rudimentary, ordered 3D structures. However, each of these techniques can only produce a specific 3D structure (i.e., hollow cylinder[33] or nanowall[34]) defined by the form of the prefabricated collector, therefore severely limiting the versatility of electrospinning as a viable additive 3D fabrication technique.

Here, we report a novel direct-write 3D electrospinning technique to construct arbitrarily shaped 3D structures in a continuous, self-aligned, fiber-by-fiber, and template-free manner. This technique is built upon the successful near-field electrospinning (NFES) technique.[35,36] To electrospin fibers at precise locations in a controlled manner, NFES is utilized due to its capacity of direct writing arbitrary 2D patterns. To stack the fibers in a consistent fiber-by-fiber manner, we turned the deposited fibers into locally fabricated "ground" to attract the subsequent fibers by using printing paper as the collector. Then, along with the predesigned path motion by a translational motion stage, controllable design and fabrication of electrospun 3D structures can be achieved. Compared with the "melt electrospinning" and "pre-fabricated ground collector" methods, this technique is more versatile, straightforward, and controllable for the precise fabrication of 3D electrospun structures.

2. EXPERIMENTAL SECTION

2.1. Materials. A 21 wt % PVDF (M_w = 534 000) solution was used at room temperature and 1 atm pressure with dimethyl sulfoxide (DMSO) and acetone as solvents, and Capstone FS-66 as an anionic surfactant unless otherwise specified. The chemicals were purchased from Sigma-Aldrich (United States) without further purification or modification.

2.2. Electrospinning. PVDF in powder form (2 g) was dispersed with 3 g of acetone for 30 min using a magnetic stirrer (Cimarec Digital Stirring Hot plates, Thermo Scientific, USA), and then 7 g of DMSO and 0.5 g of Capstone FS-66 were added into the PVDF-acetone suspension; the mixture was stirred for at least 1 h to reach a good homogeneity. A programmable *x*-*y* translational motion stage (Newport, Inc.) and a *z*-axis manual linear stage (Newport, Inc.) were combined as the 3-axis motion platform. A heavily doped silicon wafer was used as the ground plate, and a 5 cm × 5 cm printing paper (BOISE ASPEN 30, 20 lb) was used as the collector. A silicon wafer, an aluminum foil (REY 620, Reynolds, 12″ × 500 ft), and a Parafilm M (BEMIS, 01852-AB, 4″ × 250 ft) were used as reference collectors. The typical electrospinning parameters, including voltage, speed of motion stage, and spinneret-to-collector distance, were 1.0−1.8 kV, 10−90 mm/s, and 500−1000 μm, respectively corresponding to different patterns and collectors.

2.3. Structural Characterization. These electrospun 3D structures were sputter coated with gold (10 nm) using a Hummer Sputtering System (Anatech, USA) for SEM observations in a LEO 1550 Scanning Electron Microscope (LEO, Germany) or a FEI/Philips XL-30 Field Emission ESEM (FEI, Netherlands).

2.4. Electrical Measurement. An electrochemical workstation (Reference 600, Gamry Instruments, USA) was used for the transient electrical current measurements. Electrically conductive aluminum tapes (3M, 3302) were used as the electrodes.

3. RESULTS AND DISCUSSION

Figure 1a illustrates the direct-write 3D electrospinning technique, which builds on NFES. The spinneret-to-collector distance ranges from 500 μm to 2 mm, allowing deposition of fibers from the stable region of the ejected polymer jet to obtain positional accuracy. A programmable *x*−*y* translational

DOI: 10.1021/acsami.5b08909
ACS Appl. Mater. Interfaces 2015, 7, 27765−27770

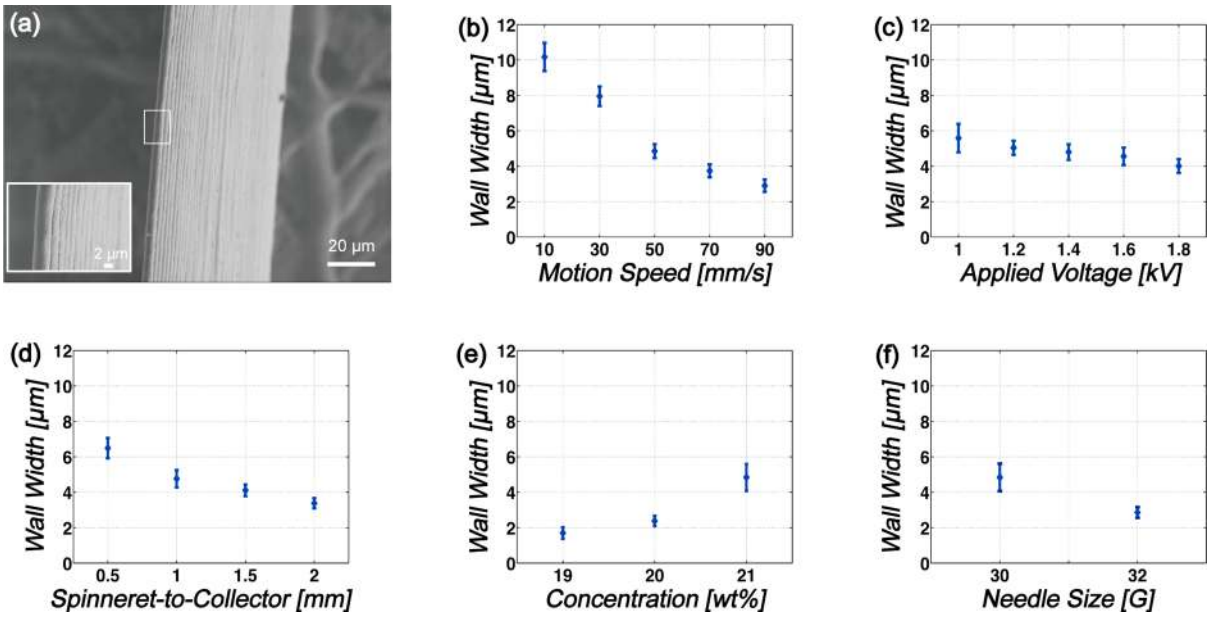

Figure 2. (a) SEM image (taken by tilting the sample by ca. 15°) of a free-standing, microwall structure made of 50 layers of electrospun fibers stacked on top of each other using this 3D electrospinning process with the spinneret size of 30 G, applied voltage at 1.5 kV, motion speed of 50 mm/s, and spinneret-to-collector distance of 1 mm. The inset shows a magnified view. (b–f) Plots showing the dependence of wall width with respect to (b) motion speed of the x–y stage, (c) applied voltage, (d) spinneret-to-collector distance, (e) polymer solution concentration, and (f) needle size. The experimental data represent the average of ten samples, with the error bars representing the distribution. The standard electrospinning process includes: motion stage speed of 50 mm/s, applied voltage at 1.5 kV, spinneret size of 30 G, spinneret-to-collector distance of 1 mm, and solution concentration of 21 wt %. Only one parameter is altered for each graph.

motion stage is used to repetitively deposit fibers, and a z-axis manual linear stage is used to adjust the spinneret-to-fiber distance. Instead of using a conventional conductive collector, a printing paper is placed on top of the grounded conductive plate to act as fibers collector. Upon landing on the collector, fibers electrospun using the NFES process generally remain wet due to the short spinneret-to-collector distance, which prevents the complete evaporation of solvent.[21,36] With the infiltration of residual solvent into the paper substrate, the local resistance of the paper in the vicinity of the deposited fiber can decrease dramatically, enhancing the electrical charge transfer between the deposited fibers and the conductive ground plate via the fibrous network within the paper (inset in Figure 1a). Such charge transfer grounds the locally deposited fibers and renders them the preferential sites for the deposition of subsequent fibers. Driven by this set of electrostatic force, the electrospun fibers can therefore be deposited in a self-aligned, consistent fiber-by-fiber manner to form arbitrarily shaped 3D structures with thin walls (Figure 1a).

Experimentally, poly(vinylidene fluoride) (PVDF) solution was used as the fiber source in the 3D electrospinning process. As a general observation, polymers that can be electrospun successfully for 3D construction have to solidify rapidly after deposition to attain a certain level of structural integrity. Otherwise, as-deposited fibers may go through undesirable processes such as reflowing, deforming, and/or fusing with other fibers. Figure 1b shows the scanning electron microscopy (SEM) image of a 3D grid structure made up of stacked PVDF fibers with average diameter ca. 8 μm. Ten single fibers were successively electrospun on top of one another with a lateral fiber-to-fiber grid pitch of 198.36 ± 13.42 μm (based on 10 measurements) while the predesigned pitch is 200 μm. Figure 1c is the close-up SEM image at the crossover location of the grid, showing orderly and spatially fiber-by-fiber depositions. Such spatial arrangement reveals a potential feature of this technology—the creation of woven electrospun meshes—that is not possible with the conventional electrospinning processes. Figure 1d shows a large-area (2 × 2 cm^2), free-standing 3D grid structure that has been physically detached from the paper substrate and was fabricated by a continuous, ca. 27 min electrospinning process with a total fiber length of ca. 40 m. The 3D grid retains its shape after detachment, showing the resilience of the grid as a structural material and the potential of a post-transfer process for further applications.

One key feature of this 3D electrospinning process is the ability to build high aspect-ratio structures. For example, a free-standing, straight wall was fabricated by consistently stacking 50 out-of-plane fibers consecutively as shown in Figure 2a of ca. 100 μm in height and ca. 5 μm in width. The width of the free-standing wall—equivalent to the diameter of a single fiber—can be altered from 1.7 ± 0.33 μm to 10.17 ± 0.8 μm by adjusting the various processing parameters. The detailed characterizations on the wall width with respect to motion speed of the x–y stage, applied voltage, spinneret-to-collector distance, polymer solution concentration, and needle size are illustrated in Figure 2b–f, respectively. Among these parameters, the speed of the motion stage appears to play the most critical role: it not only determines the wall width but also influences the fabrication accuracy of this technique. Experimental results in Figure 2b indicate that higher motion stage speed results in the reduction of wall width due to the higher mechanical drawing force. Moreover, if a suboptimal and excessive motion stage speed is chosen, the spinning fibers can lag behind the spinneret position to cause deposition error for the subsequent fibers.[21,37] Conversely, a lower motion stage speed results in piling up, buckling, and random coiling of fibers.[36,37] The 1:1 ratio between the motion stage speed and the ejection speed of the fibers is found to be the ideal condition to obtain

DOI: 10.1021/acsami.5b08909
ACS Appl. Mater. Interfaces 2015, 7, 27765–27770

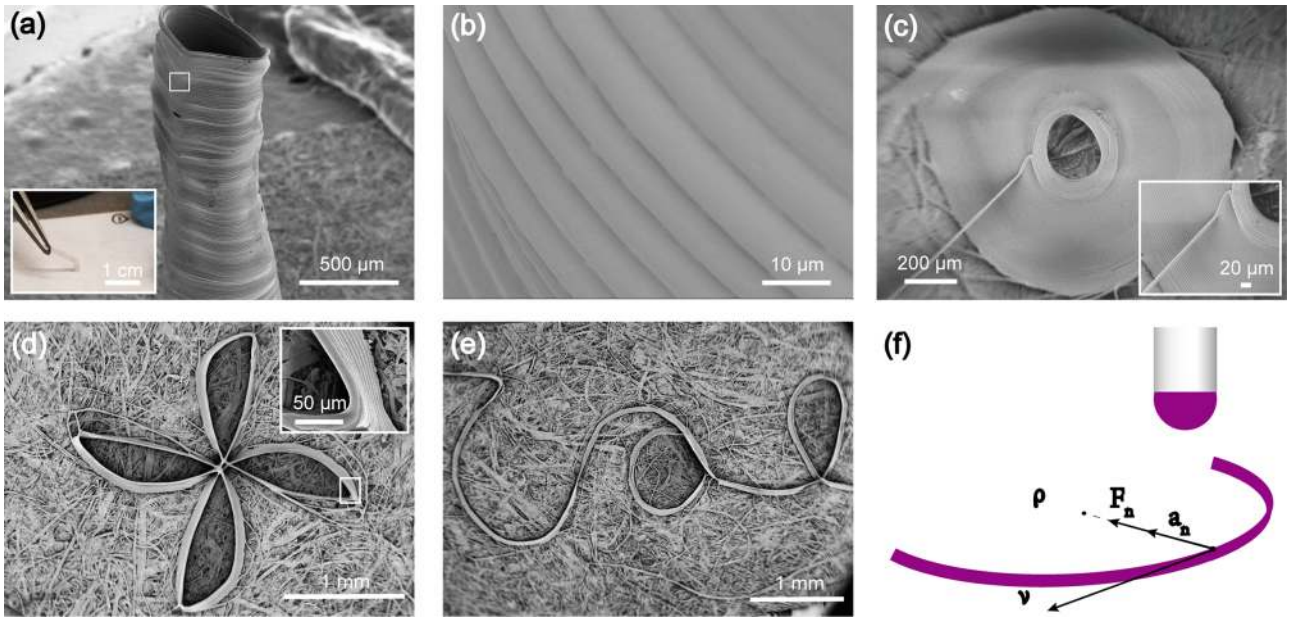

Figure 3. (a) SEM image of a cylinder made of 800 layers of electrospun fibers fabricated with the spinneret size of 30 G, applied voltage at 1.2 kV, motion speed of 10 mm/s, spinneret-to-collector distance of 1 mm, and manual *z*-axis distance control with a speed of ca. 30 μm/s. The inset shows another cylinder forcefully deformed by a tweezer. (b) SEM image of a magnified view of the sidewall in (a). (c) SEM image of a circular cone structure; the fabrication process is the same as that of (a) except without adjustment of the spinneret-to-paper distance. (d) SEM image of a 3D floral structure made of 20 layers of electrospun fibers fabricated with spinneret size of 30 G, applied voltage at 1.5 kV, motion speed of 25 mm/s, and spinneret-to-collector distance of 500 μm. (e) SEM of a 3D "*Cal*" logo with 20 layers of electrospun fibers fabricated with the same parameters as in (d). (f) Dynamics for depositing curved pattern.

morphologically and dimensionally consistent 3D structures. The fiber ejection speed can be estimated to be ca. 50 mm/s, which is determined by adjusting the speed of the motion stage such that the angle between the ejected jet and the substrate is approximately 90 deg.[21]

The controllability of this 3D electrospinning technique is demonstrated by a variety of fabricated 3D structures. Figure 3a shows a free-standing hollow cylinder made by an orderly fibers coiling and stacking process on a circular path with a radius of 250 μm for 800 cycles at a motion speed of 10 mm/s with manual adjustment of the *z*-axis linear motion stage at a speed of ca. 30 μm/s to maintain the spinneret-to-deposited structures distance. The inset of Figure 3a shows another 1.3 cm-tall hollow cylinder fabricated by the same process and forcefully tilted to about 60 degrees by a tweezer. The tube can spring back to its original shape after removing the tweezer without sustaining visible permanent deformation, highlighting strong interfacial adhesion between the fibers. The close-up SEM image (Figure 3b) shows some local corrugation-like waviness in the longitudinal direction probably caused by the perturbation of the manual *z*-axis distance control process. Without constantly adjusting the *z*-axis distance to maintain the spinneret-to-deposited structures distance, the fibers were deposited fiber-by-fiber laterally instead of vertically due to the pulling of the centripetal force as shown in Figure 3c.

In Figure 3d, we demonstrate the construction of a 3D floral structure, consisting of both arcs and straight lines. The transition regions (turning points) from straight to curved shape and vice versa (inset in Figure 3d) are relatively smooth at a motion stage speed of 25 mm/s. In Figure 3e, we further demonstrate the capability of this technique to fabricate a complicated 3D "*Cal*" logo with 20 layers of vertically stacked fibers over an area of 5 × 1.5 mm^2. One more thing needed to mention is the dynamics for depositing curvilinear fibers as shown in Figure 3f. Theoretically, during the curved deposition, the radial acceleration imposed on fibers can be expressed as $a_n = \nu^2/\rho$, where ν is the motion stage speed and ρ represents the radius of fabricated curvature. As such, when smaller radius of curvature structure is fabricated, the motion stage speed needs to be decreased so as to lower the radial acceleration and centripetal force ($F_n = m_n\ a_n$, m_n is the mass of electrospun fibers). In general, such centripetal force imposed on the electrospun fibers exerts a pulling force on the deposited pattern directed toward the center of the curvature as shown for the floral structure and "*Cal*" logo. Therefore, the building of a vertical wall for the production of 3D curved structures should be required to strike a balance between (i) careful programming of motion stage speed when electrospinning along curved paths to minimize pulling force caused by centripetal acceleration, and (ii) matching of the motion stage speed to the fibers ejection speed at around a 1:1 ratio.

The properties of the collector substrate have significant influences on the quality of the 3D electrospinning process. A 20-layer wall structure has been fabricated on different collectors, including printing paper, silicon wafer, aluminum foil, and Parafilm M film. The orderly fiber-by-fiber stacking deposition only occurs on printing paper, as illustrated in Figure 4a, whereas, for the case on the silicon and aluminum collectors, the deposited fibers experienced slippage, shrank, and even detached from substrates, resulting in failure of fiber stacking, as illustrated in Figure 4b and 4c. On the other hand, a continuous electrospinning process cannot be initiated on the Parafilm collector, leaving a totally random pattern as shown in Figure 4d.

A regular paper is typically composed of a random assembly of cellulosic fibers and some residual chemicals, and the charge transport within paper is due primarily to ion migration—ions such as sodium and chloride that are residues of the pulp

DOI: 10.1021/acsami.5b08909
ACS Appl. Mater. Interfaces 2015, 7, 27765−27770

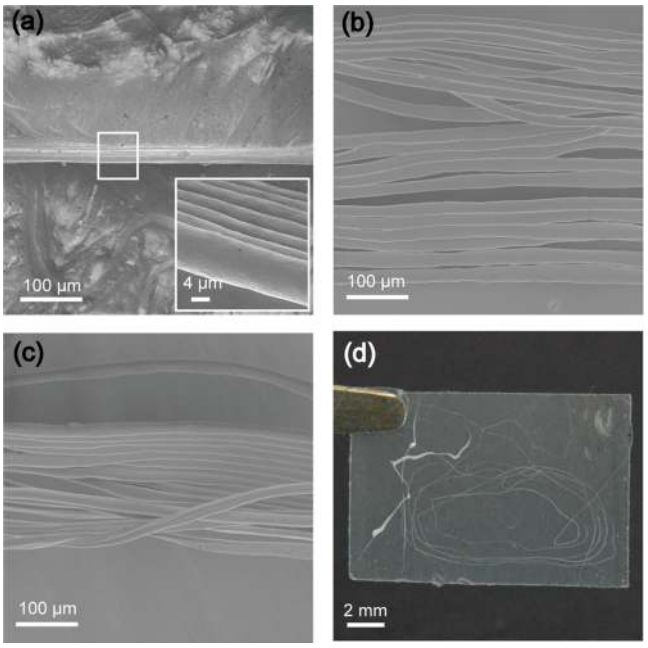

Figure 4. SEM or optical images of the 20-layer wall electrospun on different collector substrates using a 30 G needle with motion stage speed of 25 mm/s and spinneret-to-collector distance about 1 mm. The collector type and applied voltage are (a) printing paper, 1.5 kV; the inset shows the close-up view; (b) n-type silicon, 1.0 kV; (c) aluminum foil, 1.0 kV; and (d) Parafilm M film, 2.5 kV.

bleaching process—through the fibrous network.[38] It has been reported that the resistivity of paper can fall as much as 1 order of magnitude when the moisture content of the paper increases by 1% because moisture enhances ions mobility.[39] For the printing paper utilized as collector in this 3D electrospinning, the conductivity was measured by clamping the paper using two metallic electrodes connected to a DC power source. Extra care was taken to eliminate the contact resistance between the paper and electrodes by using conductive acrylic adhesive to fix them tightly. The measured conductivity is about 1×10^{-9} S/m, which is consistent with previous reports.[38,39] When ten PVDF fibers are electrospun on paper as shown in Figure 5, the conductivity increases dramatically due to infiltration of residual

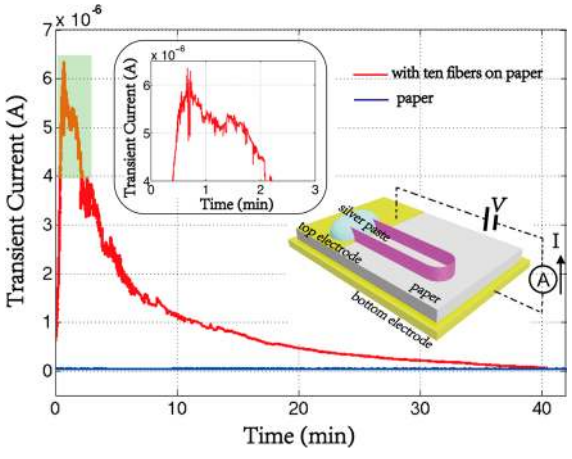

Figure 5. Two transient electrical current versus time measurements of paper (blue line) and ten PVDF electrospun fibers deposited on paper (red line) using an applied voltage of 10 V.

solvent into paper, peaking at around 2.5×10^{-4} S/m. Then, the conductivity falls slowly along with the evaporation of solvent, and it finally goes back to the original value of the paper. This is because of this unique characteristic of paper: the deposited NFES fibers can drain positive charges to the ground plate through the paper, making them as the locally fabricated electrical poles to attract the subsequent depositions of fibers. As such, the fibers are deposited in a self-aligned, consistent fiber-by-fiber manner on top of each other.

4. CONCLUSIONS

In conclusion, with a regular printing paper serving as the collector, we have successfully demonstrated a direct-write, self-aligned 3D electrospinning process. This process enables orderly fiber-by-fiber stacking to construct a variety of 3D structures in a controllable manner with designed shapes. From the perspective of manufacturing technology, this 3D electrospinning can bridge the gap between solution electrospinning and conventional 3D printing techniques. For applications, the controllable fabrication of 3D patterns on paper has the potential to promote the recently emerging technologies based on paper substrates.[40−42] In addition, the fabricated 3D structures can be conveniently detached from paper and transferred onto other substrates for subsequent treatments and applications. As such, this 3D electrospinning can be an addition to the current stage of 3D micro-/nanofabrication techoniques, and it has the potential to advance the existing electrospinning technologies in constructing 3D structures for biomedical, microelectronics, and MEMS/NMES applications.

AUTHOR INFORMATION

Corresponding Authors

*E-mail: lwlin@berkeley.edu.
*E-mail: ksteh@cal.berkeley.edu.

Author Contributions

G.L. and K.S.T. originated the original idea behind this work. G.L., K.S.T., Z.W., and L.L. conceived and designed experiments. G.L. and K.S.T. performed all the experiments. Y.L. was involved in the electrical analysis. X.Z. performed SEM and data analysis. All authors discussed the results and commented on the manuscript.

Notes

The authors declare no competing financial interest.

ACKNOWLEDGMENTS

The authors thank UC Berkeley Nanofabrication Laboratory for the experiment facilities. The authors also thank (i) Dezhi Wu and Lei Xu for helpful discussions and (ii) Caiwei Shen and Jeffrey Clarkson for assistance in taking SEM images. K.S.T. was funded by a sabbatical leave award from San Francisco State University, and G.L. was funded by the China Scholarship Council (CSC).

REFERENCES

(1) Formhals, A. Process and Apparatus for Preparing Artificial Threads. U.S. Patent 1,975,504, 1934.
(2) Dzenis, Y. Spinning Continuous Fibers for Nanotechnology. *Science* **2004**, *304*, 1917−1919.
(3) Zhang, C.-L.; Yu, S.-H. Nanoparticles Meet Electrospinning: Recent Advance and Furture Prospect. *Chem. Soc. Rev.* **2014**, *43*, 4423−4448.
(4) Reneker, D. H.; Chun, I. Nanometre Diameter Fibers of Polymer, Produced by Electrospinning. *Nanotechnology* **1996**, *7*, 216−223.

DOI: 10.1021/acsami.5b08909
ACS Appl. Mater. Interfaces 2015, 7, 27765−27770

(5) Li, D.; Xia, Y. Electrospinning of Nanofibers: Reinventing the Wheel? *Adv. Mater.* **2004**, *16*, 1151−1170.
(6) Dai, H.; Gong, J.; Kim, H.; Lee, D. A Novel Method for Preparing Ultra-Fine Alumina-Borate Oxide Fibres via an Electrospinning Technique. *Nanotechnology* **2002**, *13*, 674−677.
(7) Ramaseshan, R.; Sudarrajan, S.; Jose, R.; Ramakrishna, S. Nanostructured Ceramics by Electrospinning. *J. Appl. Phys.* **2007**, *102*, 111101.
(8) Huang, Z.-M.; Zhang, Y.-Z.; Kotaki, M.; Ramakrishna, S. A Review on Polymer Nanofibers by Electrospinning and Their Applications in Nanocomposites. *Compos. Sci. Technol.* **2003**, *63*, 2223−2253.
(9) Ko, F.; Gogotsi, Y.; Ali, A.; Naguib, N.; Ye, H.; Yang, G.; Li, C.; Willis, P. Electrospinning of Continuous Carbon Nanotube-Filled Nanofiber Yarns. *Adv. Mater.* **2003**, *15*, 1161−1165.
(10) Zhu, P.; Nair, A. S.; Peng, S.; Yang, S.; Seeram, R. Facile Fabrication of TiO_2—Graphene Composite with Enhanced Photovoltaic and Photocatalytic Properties by Electrospinning. *ACS Appl. Mater. Interfaces* **2012**, *4*, 581−585.
(11) Li, W.-J.; Laurencin, C. T.; Caterson, E. J.; Tuan, R. S.; Ko, F. K. Electrospun Nanofibrous Structures: A Novel Scaffold for Tissue Engineering. *J. Biomed. Mater. Res.* **2002**, *60*, 613−621.
(12) Huang, C.; Soenen, S. J.; Rejman, J.; Trekker, J.; Liu, C.; Lagae, L.; Ceelen, W.; Wilhelm, C.; Demeester, J.; De Smedt, S. C. Magnetic Electrospun Fibers for Cancer Therapy. *Adv. Funct. Mater.* **2012**, *22*, 2479−2486.
(13) Gopal, R.; Kaur, S.; Ma, Z.; Chan, C.; Ramakrishna, S.; Matsuura, T. Electrospun Nanofibrous Filtration Membrane. *J. Membr. Sci.* **2006**, *281*, 581−586.
(14) Ding, B.; Wang, M.; Wang, X.; Yu, J.; Sun, G. Electrospun Nanomaterials for Ultrasensitive Sensors. *Mater. Today* **2010**, *13*, 16−27.
(15) Min, S.-Y.; Kim, T.-S.; Kim, B. J.; Cho, H.; Noh, Y.-Y.; Yang, H.; Cho, J. H.; Lee, T.-W. Large-scale Organic Nanowire Lithography and Electronics. *Nat. Commun.* **2013**, *4*, 1773.
(16) Chang, J.; Liu, Y.; Heo, K.; Lee, B. Y.; Lee, S.-W.; Lin, L. Direct-Write Complementary Graphene Field Effect Transistors and Junctions via Near-Field Electrospinning. *Small* **2014**, *10*, 1920−1925.
(17) Wu, H.; Kong, D.; Ruan, Z.; Hsu, P.-C.; Wang, S.; Yu, Z.; Carney, T. J.; Hu, L.; Fan, S.; Cui, Y. A Transparent Electrode Based on a Metal Nanotrough Network. *Nat. Nanotechnol.* **2013**, *8*, 421−425.
(18) Hwang, T. H.; Lee, Y. M.; Kong, B.-S.; Seo, J.-S.; Choi, J. W. Electrospun Core-Shell Fibers for Robust Silicon Nanoparticle-Based Lithium Ion Battery Anodes. *Nano Lett.* **2012**, *12*, 802−807.
(19) Zhang, F.; Yuan, C.; Zhu, J.; Wang, J.; Zhang, X.; Lou, X. W. Flexible Films Derived from Electrospun Carbon Nanofibers Incorporated with Co_3O_4 Hollow Nanopaticles as Self-Supported Electrodes for Electrochemical Capacitors. *Adv. Funct. Mater.* **2013**, *23*, 3909−3915.
(20) Chang, C.; Tran, V. H.; Wang, J.; Fuh, Y.-K.; Lin, L. Direct-Write Piezoelectric Polymeric Nanogenerator with High Energy Conversion Efficiency. *Nano Lett.* **2010**, *10*, 726−731.
(21) Brown, T. D.; Dalton, P. D.; Hutmacher, D. W. Direct Writing by Way of Melt Electrospinning. *Adv. Mater.* **2011**, *23*, 5651−5657.
(22) Griffith, L. G.; Naughton, G. Tissue Engineering–Current Challenges and Expanding Opportunities. *Science* **2002**, *295*, 1009−1014.
(23) Shin, Y. M.; Hohman, M. M.; Brenner, M. P.; Rutledge, G. C. Experimental Characterization of Electrospinning: the Electrically Forced Jet and Instabilities. *Polymer* **2001**, *42*, 09955−09967.
(24) Teo, W. E.; Ramakrishna, S. A Review on Electrospinning Design and Nanofibre Assemblies. *Nanotechnology* **2006**, *17*, R89−R106.
(25) Greiner, A.; Wendorff, J. H. Electrospinning: A Fascinating Method for the Preparation of Ultrathin Fibers. *Angew. Chem., Int. Ed.* **2007**, *46*, 5670−5703.
(26) Hochleitner, G.; Jüngst, T.; Brown, T. D.; Hahn, K.; Moseke, C.; Jakob, F.; Dalton, P. D.; Groll, J. Additive Manufacuring of Scaffolds with Sub-micron Filaments via Melt Electrospinning Writing. *Biofabrication* **2015**, *7*, 035002.
(27) Bas, O.; De-Juan-Pardo, E. M.; Chhaya, M. P.; Wunner, F. M.; Jeon, J. E.; Klein, T. J.; Hutmacher, D. W. Enhancing Structural Integrity of Hydrogels by Using Highly Organised Melt Electrospun Fibre Constructs. *Eur. Polym. J.* **2015**, *72*, 451−463.
(28) Qin, C.-C.; Duan, X.-P.; Wang, L.; Zhang, L.-H.; Yu, M.; Dong, R.-H.; Yan, X.; He, H.-W.; Long, Y.-Z. Melt Electrospinning of Poly(lactic acid) and Polycaprolactone Microfibers by Using a Hand-operated Wimshurst Generator. *Nanoscale* **2015**, *7*, 16611−16615.
(29) Muerza-Cascante, M. L.; Haylock, D.; Hutmacher, D. W.; Dalton, P. D. Melt Electrospinning and Its Technologization in Tissue Engineering. *Tissue Eng., Part B* **2015**, *21*, 187−202.
(30) Visser, J.; Melchel, F. P.W.; Jeon, J. E.; van Bussel, E. M.; Kimpton, L. S.; Byrne, H. M.; Dhert, W. J.A.; Dalton, P. D.; Hutmacher, D. W.; Malda, J. Reinforcement of Hydrogels Using Three-Dimensionally Printed Microfibres. *Nat. Commun.* **2015**, *6*, 6933.
(31) Brown, T. D.; Edin, F.; Detta, N.; Skelton, A. D.; Hutmacher, D. W.; Dalton, P. D. Melt Electrospinning of Poly(ε-caprolactone) Scaffolds: Phenomenological Observations Associated with Collection and Direct Writing. *Mater. Sci. Eng., C* **2014**, *45*, 698−708.
(32) Ristovski, N.; Bock, N.; Liao, S.; Powell, S. K.; Ren, J.; Kirby, G. T. S.; Blackwood, K. A.; Woodruff, M. A. Improved Fabrication of Melt Electrospun Tissue Engineering Scaffolds Using Direct Writing and Advanced Electric Field Control. *Biointerphases* **2015**, *10*, 011006.
(33) Kim, H.-Y.; Lee, M.; Park, K. J.; Kim, S.; Mahadevan, L. Nanopottery: Coiling of Electrospun Polymer Nanofibers. *Nano Lett.* **2010**, *10*, 2138−2140.
(34) Lee, M.; Kim, H.-Y. Toward Nanoscale Three-Dimensional Printing: Nanowalls Built of Electrospun Nanofibers. *Langmuir* **2014**, *30*, 1210−1214.
(35) Sun, D.; Chang, C.; Li, S.; Lin, L. Near-field Electrospinning. *Nano Lett.* **2006**, *6*, 839−842.
(36) Chang, C.; Limkrailassiri, K.; Lin, L. Continuous Near-field Electrospinning for Large Area Deposition of Orderly Nanofiber Patterns. *Appl. Phys. Lett.* **2008**, *93*, 123111.
(37) Blount, M. J.; Lister, J. R. The Asymptotic Structure of a Slender Dragged Viscous Thread. *J. Fluid Mech.* **2011**, *674*, 489−521.
(38) Josefowicz, J. Y.; Deslandes, Y. Electrical Conductivity of Paper: Measurement Methods and Charge Transport Mechanisms. In *Colloids and Surfaces in Reprographic Technology*; Hair, M., Croucher, M. D., Eds.; *ACS Symposium Series*; American Chemical Society: Washington, DC, 2005; pp 493−530.
(39) Mark, R. E.; Habeger, C. C.; Borch, J.; Lyne, M. B. *Handbook of Physical Testing of Paper*; Marcel Dekker: New York, 2002; pp 375−385.
(40) Martinez, A. W.; Phillips, S. T.; Butte, M. J.; Whitesides, G. M. Patterned Paper as a Platform for Inexpensive, Low-Volume, Portable Bioassays. *Angew. Chem., Int. Ed.* **2007**, *46*, 1318−1320.
(41) Hu, L.; Wu, H.; Mantia, F. L.; Yang, Y.; Cui, Y. Thin, Flexible Secondary Li-ion Paper Batteries. *ACS Nano* **2010**, *4*, 5843−5848.
(42) Liu, X.; Mwangqi, M.; Li, X.; O'Brien, M.; Whitesides, G. M. Paper-based Piezoresistive MEMS Sensors. *Lab Chip* **2011**, *11*, 2189−2196.

DOI: 10.1021/acsami.5b08909
ACS Appl. Mater. Interfaces 2015, 7, 27765−27770